Mechanistic Studies on the Coupled Reaction of *n*-Hexane and Ethanol Over HZSM-5 Zeolite Catalyst

Jinlong Wan · Fuxiang Chang · Yingxu Wei · Qinghua Xia · Zhongmin Liu

Abstract The coupled reaction of *n*-hexane and ethanol over HZSM-5 zeolite has been, for the first time, investigated with a pulse-reaction system. The catalytic reaction results showed an improvement of the initial conversion activity of *n*-hexane when ethanol was introduced as co-reactant. The FT-IR analysis revealed that the ethanol molecules adsorbed on Brønsted acidic sites were immediately transformed into surface ethoxy groups, which were active species for converting *n*-hexane and improving the initial conversion activity of *n*-hexane by a bimolecular hydride transfer mode. Also, the catalytic tests suggested that alkenes resulting from the transformation of ethanol could not enhance the initial conversion of *n*-hexane compared to active ethoxy groups at the shortest contact time. A mechanism involving the ethoxy groups was proposed to understand the coupled reaction of ethanol and *n*-hexane.

Keywords *n*-Hexane · Ethanol · HZSM-5 · Coupled reaction · Mechanism

J. Wan · F. Chang · Y. Wei · Q. Xia · Z. Liu (✉)
Natural Gas Utilization and Applied Catalysis Laboratory,
Dalian Institute of Chemical Physics, Chinese Academy of
Sciences, P.O. Box 110, 116023 Dalian,
People's Republic of China
e-mail: Liuzm@dicp.ac.cn

J. Wan
Graduate School of the Chinese Academy of Sciences,
Beijing 100039, People's Republic of China

Q. Xia
Ministry-of-Education Key Laboratory for the Synthesis and
Application of Organic Functional Molecules, Hubei University,
Wuhan 430062, People's Republic of China

1 Introduction

The demand for light olefins in petrochemical industries has been increasing day by day. At present, most light olefins are obtained from thermal cracking of naphtha and light alkanes. These are very energy-consuming and high-cost processes. Both catalytic cracking of naphtha [1, 2] and catalytic transformation of methanol [3, 4] to olefins on solid acid catalysts have been developed as alternative processes to meet the increasingly demand for light alkenes. These two resources are evidently characterized by the opposite heat effects and the same solid acid catalysts. Taking into account the energy balance and the yield enhancement of target products, the effective combination of endothermic hydrocarbon cracking with exothermic methanol conversion will show a promising route to obtain the desired light alkenes with much less energy cost.

It has been shown that the coupled conversion of hydrocarbon and methanol could obtain a high yield of olefins in a nearly thermo-neutral condition [5]. The other works have been performed in this field; e.g. Gao et al. [6] investigated the coupled conversion of methanol and C$_4$ hydrocarbons over zeolite catalyst at moderate temperatures; Shabalina et al. [7] also studied the methanol-coupled conversion of propane and butane on MFI zeolite. However, besides the consideration of energy supply, above studies emphasized the importance of reaction condition and zeolite catalyst for higher yield of light olefins. No report has approached the mechanism of such a coupled reaction. Despite the fact that the conversion of both reactants are quite different and complicated [8–12], the mechanism investigation of the coupled reaction will enable us to understand the reaction process and to develop the catalysts.

We previously investigated the coupled reaction of *n*-hexane and methanol over HZSM-5 zeolites [13], and found an improved conversion activity of *n*-hexane and an increased contribution of faster bimolecular mechanism to the *n*-hexane conversion by methanol. Furthermore, our recent work on this coupled system [14] has shown how the intermediates and products from the methanol acted as the active species for the initial activation and chain propagation of *n*-hexane and how the *n*-hexane in the coupled system accelerated the conversion of methanol. Despite the proposed possible reaction mechanism of the coupled reaction system would allow us to understand the system to some extent, the validity and universality of the mechanism still need to be further studied in order to obtain the valuable mechanistic insight.

In this work the ethanol coupled *n*-hexane cracking was tested and compared with the individual reactions such as *n*-hexane and ethanol conversions. A FT-IR technique was applied to determine the intermediate species resulting from ethanol adsorbed on zeolite, and a detailed initial activation route of *n*-hexane in the coupled reaction was discussed.

2 Experimental

2.1 Catalytic Test

HZSM-5 (Si/Al = 19, from NanKai University, China) was employed as the catalyst in this work. The catalytic experiments were performed at atmospheric pressure on a pulse reaction system equipped a VARIAN CP-3800 gas chromatograph (GC) with a 6-way valve and a 10-way valve, which had been described previously [14]. The flow chart of the pulse reaction system given in Fig. 1 described how reactant gases were mixed in the correct proportions to compose the inlet stream. The *n*-hexane vapor was generated by passing He flow through a saturator at proper temperature. This stream was then mixed with the ethanol stream generated in the same way, and then the mixed stream was continuously passed through the 6-way valve. The reactant pulse could be injected into the reactor by the 10-way valve. After eluting the reactor, the reacted pulse was introduced to the GC equipped with a capillary column (PONA, 100 m × 0.25 mm) and a FID detector for product analysis. The conversion of the reactants and the yield of products were expressed on a molar carbon atom basis as described elsewhere [14]. And the contact time could be calculated with the equation:

$$\text{Contact time} \ = \ V_{cat}/F_{gas},$$

where V_{cat} and F_{gas} represents the volume of catalyst bed and the injecting flow rate of He flow, respectively.

2.2 FT-IR Studies of Ethanol Adsorption at Different Temperatures

FT-IR spectra of ethanol adsorption on HZSM-5 zeolite at different temperatures were recorded on a Bruker EQUINOX 55 FT-IR spectrometer with a resolution of 4 cm^{-1} and 32 scans. The HZSM-5 zeolite sample wafer was activated at 400 °C for 4 h in a quartz cell under vacuum. Ethanol vapor was introduced into the IR cell to contact zeolite wafers for 10 min at a certain temperature for saturated adsorption. Then the IR cell was further evacuated for 20 min at the same temperature to remove excess ethanol in the cell before the spectra were recorded. Difference spectra were obtained by subtracting the spectra before and after adsorption at the same temperature.

Fig. 1 Schematic representation of catalytic reaction. (I) Six-way valve of CP-3800. (II) Ten-way valve of CP-3800
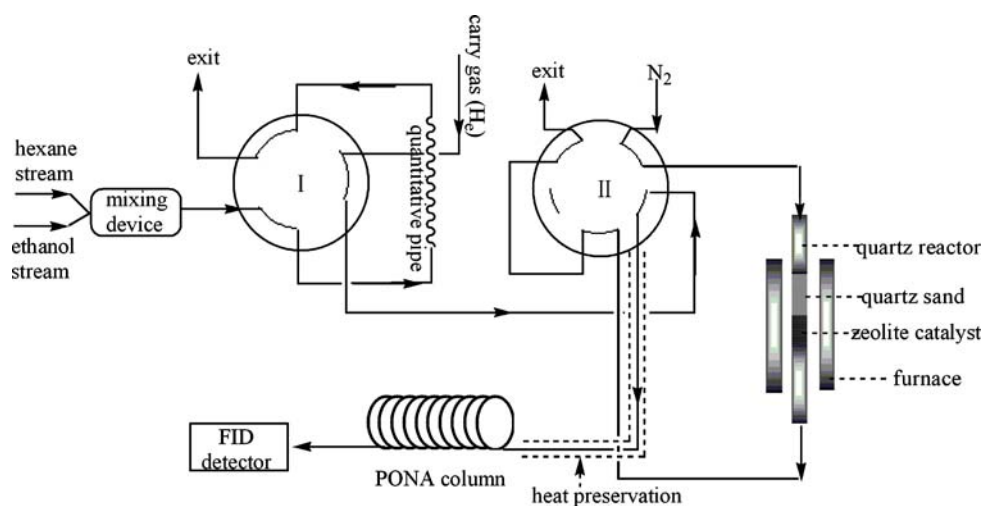
3 Results and Discussion

3.1 Coupled Transformation of *n*-Hexane and Ethanol at 400 °C

In our previous researches [13, 14], it was observed that the introduction of methanol improved the conversion of *n*-hexane in the coupled system. Similarly, the coupled transformations of *n*-hexane and ethanol, as well as the uncoupled transformations of *n*-hexane, were performed over HZSM-5 catalyst at 400° C at different contact times. The coupled conversion of *n*-hexane is evidently higher than the uncoupled one (Fig. 2) over a large range of contact times 0.00283–0.00864 s. The ratio of ethanol-coupled *n*-C$_6$ conversion to uncoupled *n*-C$_6$ conversion, characteristic of the effect of ethanol introduction, became larger with the decrease of the contact time, which strongly suggested that the introduction of ethanol could enhance the initial activation of *n*-hexane conversion.

In addition, ethanol always showed a complete conversion of 100% even at the shortest contact times employed in the coupled reaction (not shown in Fig. 2). The easy-conversion of ethanol indicates that ethanol molecules are first transformed into intermediate species on the acid sites. This can be readily understood in term of the energy difference of 111 kJ/mol between the proton affinities of *n*-hexane and ethanol as listed in Table 1 [15, 16], which predicts the stronger bonding between ethanol and hydroxy group. Thus, the enhanced initial conversion activity of *n*-hexane is probably attributed to the ethanol transformation in the coupled system prior to the adsorption and conversion of *n*-hexane, which means that the intermediate species or products from the ethanol conversion could be responsible for such an enhancement.
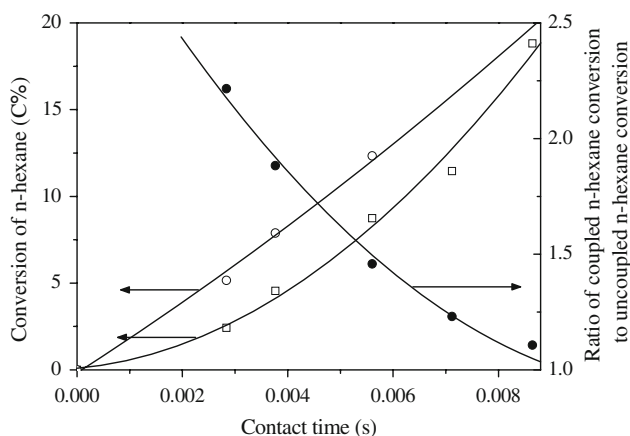
Table 1 Proton affinities of two kinds of feed

Compound	*n*-hexane	Ethanol
Proton affinity (KJ/mol)	665[a]	776[b]

[a] Taken from ref. [16]

[b] Taken from NIST Chemistry WebBook

3.2 FT-IR Studies of the Adsorption of Ethanol on the Activated HZSM-5 Zeolite

FT-IR measurements of ethanol adsorption upon the activated HZSM-5 zeolite were carried out in order to determine the formation of surface species when ethanol was adsorbed on HZSM-5 in the temperature range of 25–250 °C. Figure 3 shows the difference spectra of ethanol adsorption on HZSM-5 zeolite at different temperatures. At room temperature (Fig. 3a), ethanol was adsorbed on HZSM-5 zeolite through interacting with three types of hydroxyl groups (namely terminal silanol groups, AlOH groups and the bridging hydroxyls) to result in three negative absorbances at 3,745, 3,670 and 3,614 cm^{-1} [17–20]. Furthermore, the adsorption on bridging hydroxyl groups (Fig. 3a) also gives rise to a broad band at 3,555 cm^{-1}. This band can be assigned to the OH vibrations of the hydrogen-bonded ethanol [20–25]. At the same time, some new bands could also be observed at 2,982, 2,937, 1,448 and 1,395 cm^{-1} (Fig. 3a). These bands can be assigned to symmetric and asymmetric vibrations of the CH$_3$ groups in the adsorbed ethanol, while the bands at 2,963, 2,905, 2,877 and 2,851 cm^{-1} can be due to symmetric and asymmetric vibrations of the CH$_2$ groups [20, 22–25]. When the temperature was increased from 25 to 100 °C, the bands at 3,745 and 3,670 cm^{-1} disappeared

Fig. 2 Conversions of *n*-hexane without ethanol coupling (□) and with ethanol coupling (○) and ratio of coupled *n*-C$_6$ conversion and uncoupled *n*-C$_6$ conversion (●) versus contact time at 400 °C over HZSM-5 zeolite (Si/Al = 19)
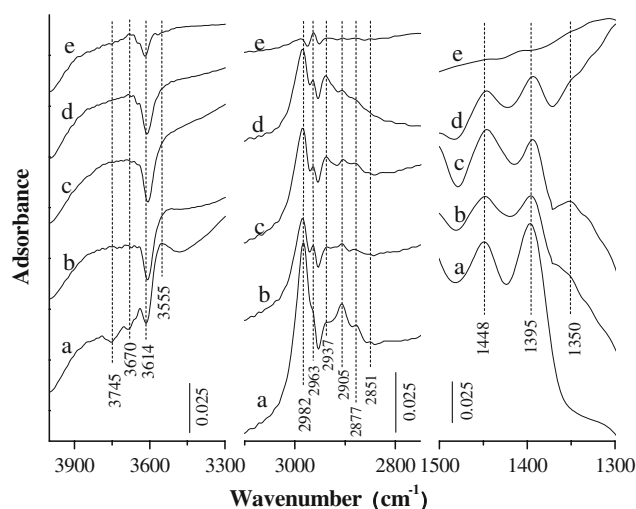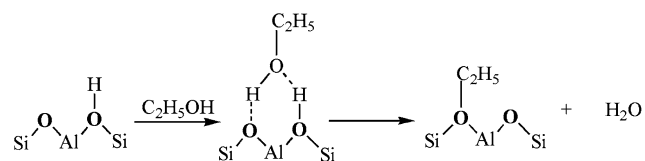

Fig. 3 Infrared difference spectra recorded after the adsorption of ethanol on HZSM-5 zeolite at **a** 25 °C, **b** 100 °C, **c** 150 °C, **d** 200 °C, **e** 250 °C

(Fig. 3b). According to the proposals made by Natal-Santiago et al. [25] and Decanio et al. [26], these bands could be caused by weakly physisorbed ethanol and easily removed from the acid surface with the increase of temperature. In addition, the intensity of the 3,555 cm^{-1} band decreased, accompanied by the appearance of one new band at 1,350 cm^{-1} due to the formation of H$_2$O at 100 °C [27, 28]. This evolution can be attributed to the dehydration of hydrogen-bonded ethanol to produce water, in good agreement with the results reported by Kondo et al. [24]. Figure 3c shows that at 150 °C the band at 3,555 cm^{-1} disappears, while one at 1,350 cm^{-1} is intensified, which suggests that the dehydration reaction of adsorbed ethanol is much more prominent at 150 °C. In the same spectrum, the bands at 3,000–2,800 cm^{-1} due to vibrations of the CH$_2$ groups are still visible. Therefore, the steady intermediate from ethanol dehydration on zeolite can be identified as an ethoxy group at 150 °C as described in Scheme 1 [24].

With a further increase of temperature to higher than 150 °C, the intensity of the bands at 3,000–2,800 cm^{-1} due to vibrations of the CH$_2$ groups decreased, accompanied by the disappearance of the band at 1,350 cm^{-1} (Fig. 3d, e), but the band at 3,614 cm^{-1} due to the interaction of the Brønsted acid sites with ethanol was still present at the same temperature, indicative of the complete transformation of the adsorbed ethanol into the surface ethoxy groups at relatively high temperature.

3.3 The Effect of Ethanol Transformation on the Conversion of *n*-Hexane

To investigate the major products from ethanol transformation, the uncoupled conversion of ethanol was performed over HZSM-5 catalyst at 400 °C with different contact times. The results in Fig. 4 show that the selectivity of ethene product displays a rapid increase with the decrease of the contact time, and may reach 100% at zero contact time. This suggests that the dehydration of ethanol to produce ethene is the only reaction occurring at the shortest contact time. However, our previous investigation [14] suggested that ethene could not promote the initial activation of *n*-hexane in the coupled system, attributable to the difficult formation of primary ethylcarbenium ion from ethene [11, 12, 29]. Therefore, the improvement of

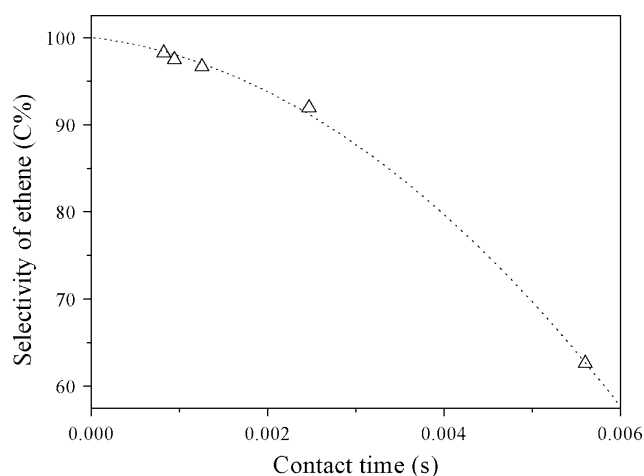**Fig. 4** Selectivity of ethene versus contact time for ethanol transformation at 400 °C over HZSM-5 zeolite (Si/Al = 19)

the initial conversion activity of *n*-hexane might be contributed by the adsorbed intermediate species arising from the transformation of ethanol on the zeolite. The infrared measurements of ethanol adsorbed on the HZSM-5 zeolite catalyst suggested that the adsorbed intermediate species were surface ethoxy groups after ethanol was contacted with the activated zeolite at 100–250 °C, where the surface ethoxy groups acted as active species. By analogy with the ionic characteristic of methoxy groups at higher temperature, it seems more likely that the ethoxy groups (as the transition states) behaved as partly positive-charged carbenium ions at high reaction temperature [30–32], to activate *n*-hexane molecules more readily than the Brønsted acid sites on the zeolite surface.
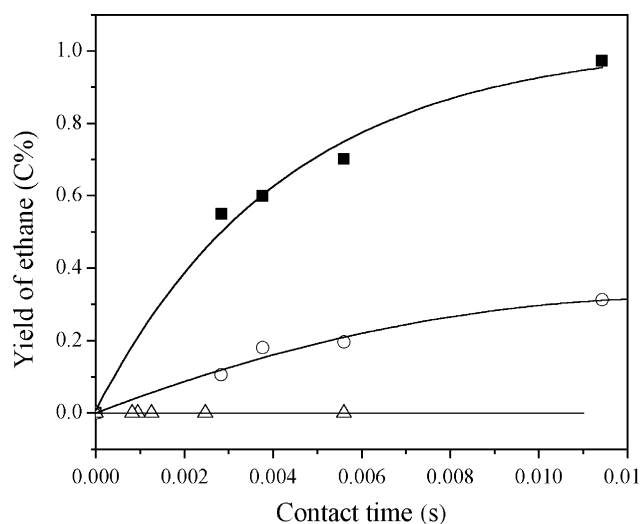

Fig. 5 Yield of ethane versus contact time for *n*-hexane conversion with ethanol coupling (■), the conversion of *n*-hexane alone (○), and the conversion of ethanol (△) at 400 °C over HZSM-5 zeolite (Si/Al = 19)

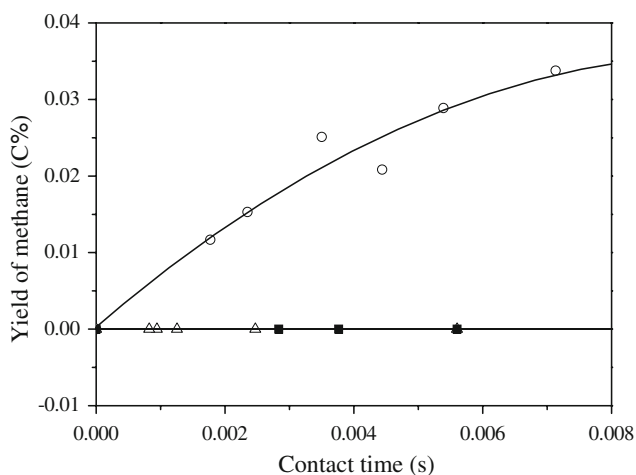**Scheme 1** Mechanism of ethanol dehydration on zeolite

Fig. 6 Yield of methane versus contact time for *n*-hexane conversion with ethanol coupling (■), the conversion of *n*-hexane alone (○), and the conversion of ethanol (△) at 400 °C over HZSM-5 zeolite (Si/Al = 19)
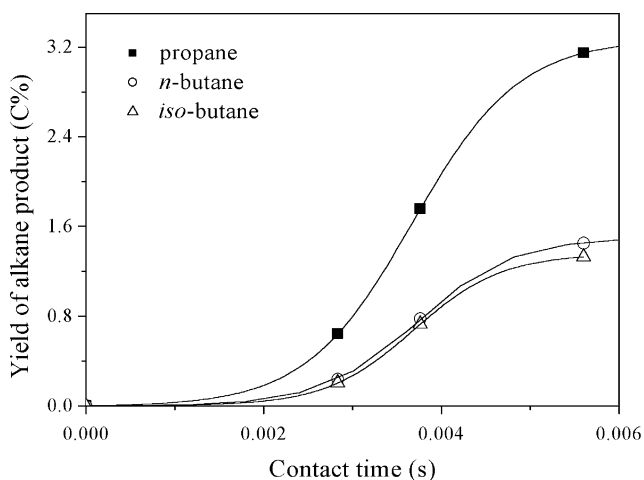

Fig. 7 Yields of C_3–C_4 alkane products versus contact time for *n*-hexane conversion with ethanol coupling at 400 °C over HZSM-5 zeolite (Si/Al = 19)

3.4 Proposed Reaction Pathway of *n*-Hexane Activation with Ethanol as Co-reactant

The catalytic results from the coupled transformations of *n*-hexane and ethanol as well as the transformations of the individual reactants indicate the difference in the initial formation rates of ethane and methane. Figure 5 shows that the initial formation rates of ethane (estimated from curve slopes at the zero contact time) were different in three reaction systems. It is obvious that the initial formation rate of ethane in the coupled system was much higher than those in the individual reactant systems. As noted above, ethene could not promote the initial activation of *n*-hexane in the coupled system, meaning that only ethoxy group was responsible for the highest initial formation rate of ethane product in the coupled system. Figure 6 shows that methane was only detected in the uncoupled reaction of *n*-hexane, indicating that the monomolecular protonation reaction could not occur in the coupled system [10, 12, 32–37]. Therefore, the interaction of ethoxy groups with *n*-hexane quite likely occurred through the hydride transfer reaction to form ethane product. This was in accordance with the results reported by Houriet et al. [34], who considered that the interaction between ethoxy groups and alkanes could merely occur through the hydride transfer reaction.

Also, the initial formation rates of the C_3–C_4 alkanes in the coupled transformations of *n*-hexane and ethanol (estimated from curve slopes at the zero contact time) are shown in Fig. 7. It is obvious that the initial formation rates of the C_3–C_4 alkanes tended to be zero at the shortest contact time, which suggested that the bimolecular hydrid transfer reaction between C_3 and C_4 alkenes and *n*-hexane could not occur in the initial activation of *n*-hexane. Thus, it can come to the conclusion that only the ethoxy groups resulting from ethanol notably improved the initial activation of *n*-hexane through a hydride transfer reaction in the coupled system.

These results further allowed us to propose the following reaction mechanism on the coupled reaction of ethanol and

Scheme 2 An adsorbed ethoxy species derived from ethanol occuring in two possible reaction ways in the coupled system. **a** Activating the feed *n*-hexane molecule through the bimolecular H- transfer route. **b** The direct desorption from Brønsted acid sites on the zeolite surface
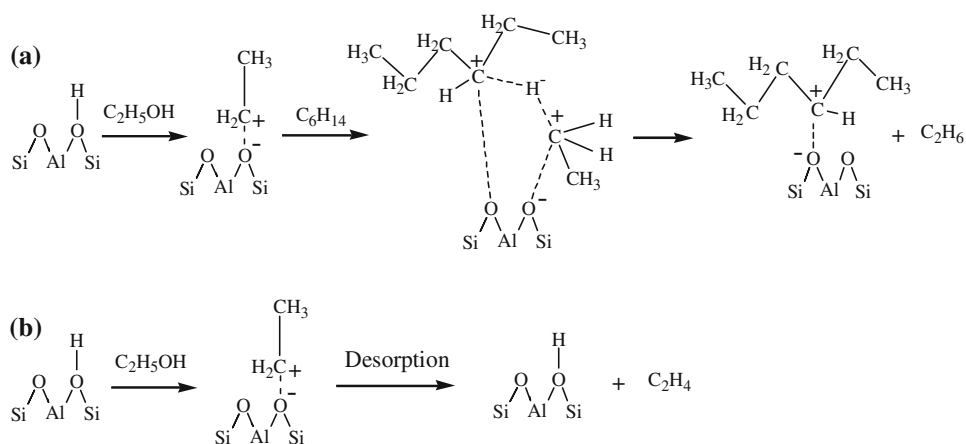
n-hexane. Firstly, ethanol was adsorbed on active sites and transformed into surface ethoxy groups prior to *n*-hexane. Once the ethoxy group was formed, it could further interact with *n*-hexane or be directly desorbed. The interaction of ethoxy groups and *n*-hexane would secondly initiate the conversion of *n*-hexane through a bimolecular hydride transfer with an attack of *n*-hexane by the surface ethoxy groups. As shown in Scheme 2a, such an attack could result in the stretching and strong polarization of the C–O bond as well as the formation of the adsorbed nonclassical carbonium ion $[C_6H_{13}–H–C_2H_5]^+$, which would subsequently decompose to release an ethane molecule and a carbenium ion $[C_6H_{13}]^+$. As a result, the introduction of ethanol could largely enhance the initial activation of *n*-hexane, while the direct desorption of ethoxy groups would lead to the formation of plentiful ethene products (Scheme 2b) [24].

4 Conclusion

A higher initial conversion rate of *n*-hexane was obtained when ethanol was used as co-reactant by the pulse catalytic system. IR spectroscopy showed the direct formation of ethoxy groups as steady intermediates on the zeolite during ethanol adsorption on Brønsted acidic sites. The catalytic tests suggested that ethene was only a product resulting from the dehydration of ethanol over the zeolite catalyst at the shortest contact time, which could not enhance the initial conversion of *n*-hexane. The initial formation rates of ethane were improved with the participation of ethanol into the reaction.

A mechanism route has been proposed to explain the possible reaction route of this coupling reaction system. The intermediate ethoxy group species (from the ethanol transformation on zeolite active sites) could be responsible for the initial activation of *n*-hexane *via* a bimolecular hydride transfer. Together with the effect of methoxy groups from methanol on the initial activation of *n*-hexane, we can conclude that alkoxy groups could indeed activate *n*-hexane molecules in the coupled reaction, which further extended the application scope of our investigations on the mechanisms.

References

1. Wei YX, Liu ZM, Wang GW, Qi Y, Xu L, Xie P, He YL (2005) Stud Surf Sci Catal 158:1223–1230
2. Yoshimura Y, Matano K, Mizukami F, Shokubai (2001) Stud Surf Sci Catal 43(3):218–223
3. Chang CD, Silvestri AJ (1977) J Catal 47:249–259
4. Chang CD (1983) Catal Rev Sci Eng 25:1–118
5. Lűcke B, Martin A (1999) Microporous Mesoporous Mater 29:145–157
6. Gao ZX, Cheng RC, Tan YC, Zhu QH (1995) J Fuel Chem Tech 23(4):349–354
7. Erofeev VL, Shabalina LB, Koval LM, Minakova TS (2002) Russ J Appl Chem 75(12):752–754
8. Stöcker M (1999) Microporous Mesoporous Mater 29:3–48
9. Haw JF, Song WG, Marcus DM, Nicholas JB (2003) Acc Chem Res 36:317–326
10. Corma A, Orchillés AV (2000) Microporous Mesoporous Mater 35–36:21–30
11. VY Kissin (2001) Catal Rev Sci Eng 43(1&2):85–147
12. Jentoft FC, Gates BC (1997) Top Catal 4:1–13
13. Chang FX, Wei YX, Liu XB, Qi Y, Zhang DZ, He YL, Liu ZM (2006) Catal Lett 106:171–176
14. Chang FX, Wei YX, Liu XB, Zhao YF, Xu L, Sun Y, Zhang DZ, He YL, Liu ZM (2007) Appl Catal A Gen 328:163–173
15. Sowerby B, Becker SJ, Belcher LJ (1996) J Catal 161:377–386
16. Haw JF (2002) Phys Chem Chem Phys 4:5431–5441
17. Forester TR, Howe RF (1987) J Am Chem Soc 109:5076–5082
18. Kubelková L, Nováková J, Nedomová K (1990) J Catal 124:441–450
19. Campbell SM, Jiang XZ, Howe RF (1999) Microporous Mesoporous Mater 29:91–108
20. Golay S, Doepper R, Renken A (1998) Appl Catal A 172:97–106
21. Larsen G, Lotero E, Márquez M, Silva H (1995) J Catal 157:645–655
22. Knözinger H, Stübner B (1978) J Phys Chem 82(13):1526–1532
23. Schenkel R, Jentys A, Parker SF, Lercher JA (2004) J Phys Chem B 108:15013–15026
24. Kondo JN, Ito K, Yoda E, Wakabayashi F, Domen K (2005) J Phys Chem B 109:10969–10972
25. Natal-Santiago MA, Dumesic JA (1998) J Catal 175:252–268
26. Decanio EC, Nero VP, Bruno JW (1992) J Catal 135:444–457
27. Pazé C, Bordiga S, Lamberti C, Salvalaggio M, Zecchina A (1997) J Phys Chem B 101:4740–4751
28. Hadjiivanov K, Saussey J, Freysz JL, Lavalley JC (1998) Catal Lett 52:103–108
29. Anderson BG, Schumacher RR, van Duren R, Singh AP, van Santen RA (2002) J Mol Catal A 181:291–301
30. Ono BY, Mori T (1981) J Chem Soc Faraday Trans 77:2209–2221
31. Kazansky VB, Senchenya IN (1989) J Catal 119:108–120
32. Hutchings GJ, Watson GW, Willock DJ (1999) Microporous Mesoporous Mater 29:67–77
33. Clow RP, Futrell JH (1972) J Am Chem Soc 94:3748–3755
34. Houriet R, Parisod G, Gäumann T (1977) J Am Chem Soc 99:3599–3602
35. Mark S, Schellhammer C, Niedner-Schatteburg G, Gerlich D (1995) J Phys Chem 99:15587–15594
36. Kazansky VB, Frash MV (1994) Catal Lett 28:211–222
37. Kazansky VB, Frash MV, van Santen RA (1997) Catal Lett 48:61–67